2.3 Geophysical Investigations

2.3.1 Aims

- To identify potential water-conducting features and impermeable argillaceous layers.
- To acquire information on the orientation and geometry of geological discontinuities.
- To acquire geophysical properties by continuous wire line logging to support the geological and hydrochemical modelling.
- To characterise in situ neutron flux production for hydrochemical interpretations.

2.3.2 Work performed

Geophysical logging: A suite of borehole geophysical logging methods, consisting of temperature, spontaneous potential, resistivity, micro-resistivity, natural gamma, gamma spectrum, neutron, density, acoustic, X-Y calliper and deviation logging methods were employed from the surface to the bottom of each borehole. In MSB-1, because the groundwater level in the borehole was below 60 mabh, geophysical logging was conducted in an injection state above the static water level.

BTV: BTV investigations were performed from the surface to the bottom of each borehole. Below 92 mabh in MSB-3, the BTV investigation was performed through PQ rods installed to the depth as casing pipe, because borehole collapse had occurred during drilling in the interval from 91 to 102 mabh near the NNW fault.

2.3.3 Results

Geophysical logging:

- Continuous profiles of the geophysical properties were acquired from the surface to the bottom of each borehole. Geophysical logs are presented in Figures 21, 22, 23 and 24.
- Conglomerate layers and coarse sandstone layers intercalated in the Akeyo Formation and the Toki Lignite-bearing Formation and the unconformity between the Mizunami Group and the Toki Granite are distinct anomalies on the spontaneous potential, resistivity, micro-resistivity, neutron, acoustic and density logs. Although these coarse clastic layers in the sedimentary formations are generally inferred to be permeable, the depths at which distinct anomalies on the geophysical logs occurred are not always coincident with fluid loss zones and anomalies identified by fluid logging (Figures 21, 22, 23 and 24, see section **2.4.3** for relevant matters).
- Relatively high gamma anomalies (500 to 2,000 API above background) were identified in the arkosic sandstone immediately above the basal conglomerate of the Toki-Lignite bearing Formation in MSB-1, 2 and 3, and immediately above the unconformity between the Mizunami Group and the Toki Granite in MSB-4.
- The tuffaceous sandstone and tuff layers above the top of the basal conglomerate and below the mudstone or muddy sandstone in the Akeyo Formation were defined as low resistivity sections in each borehole. According to the study in the Tono Mine area [6], the sections are possibly impermeable layers in the sedimentary rocks.

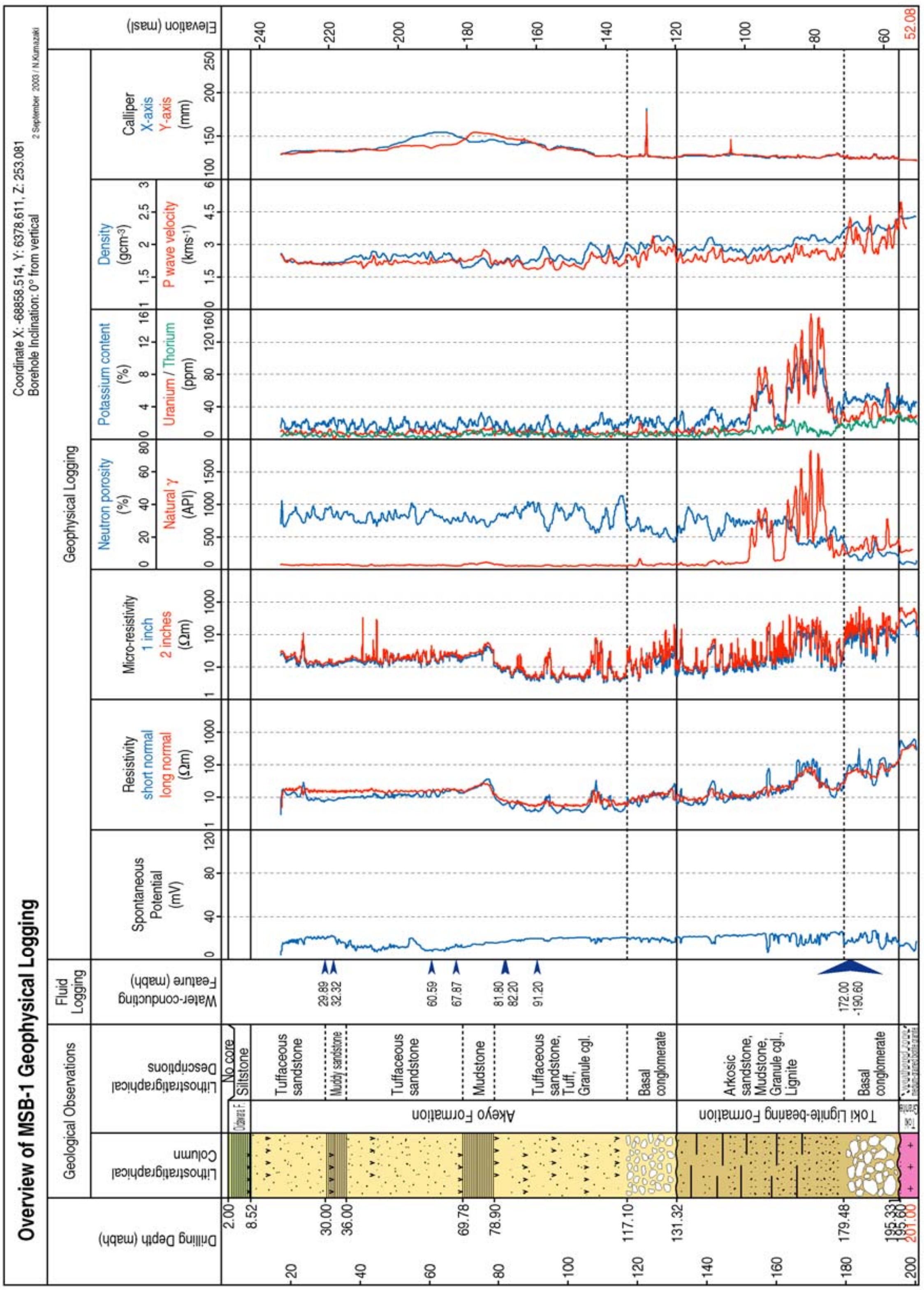

Figure 21 Overview of MSB-1 geophysical logging

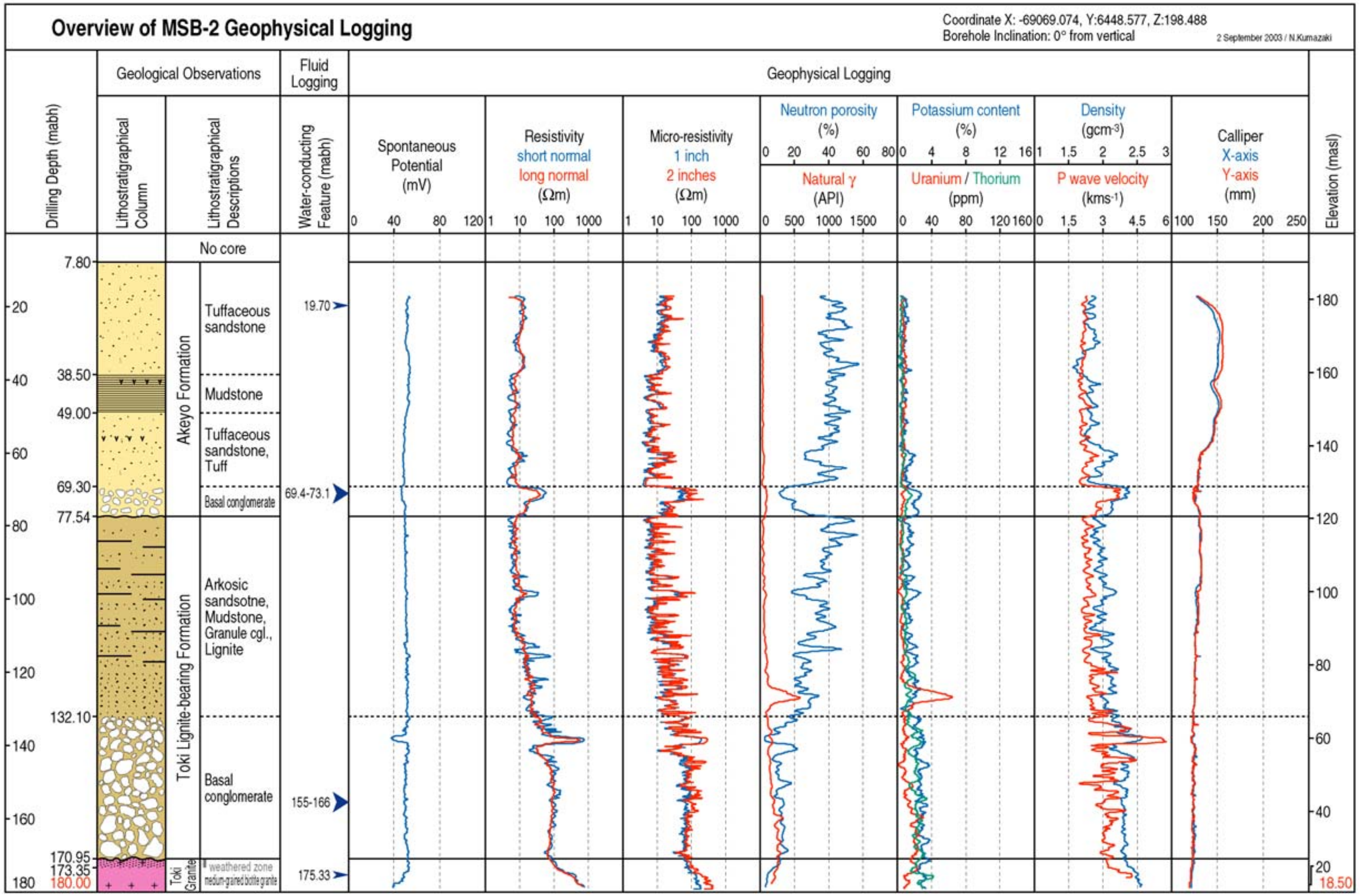

Figure 22 Overview of MSB-2 geophysical logging

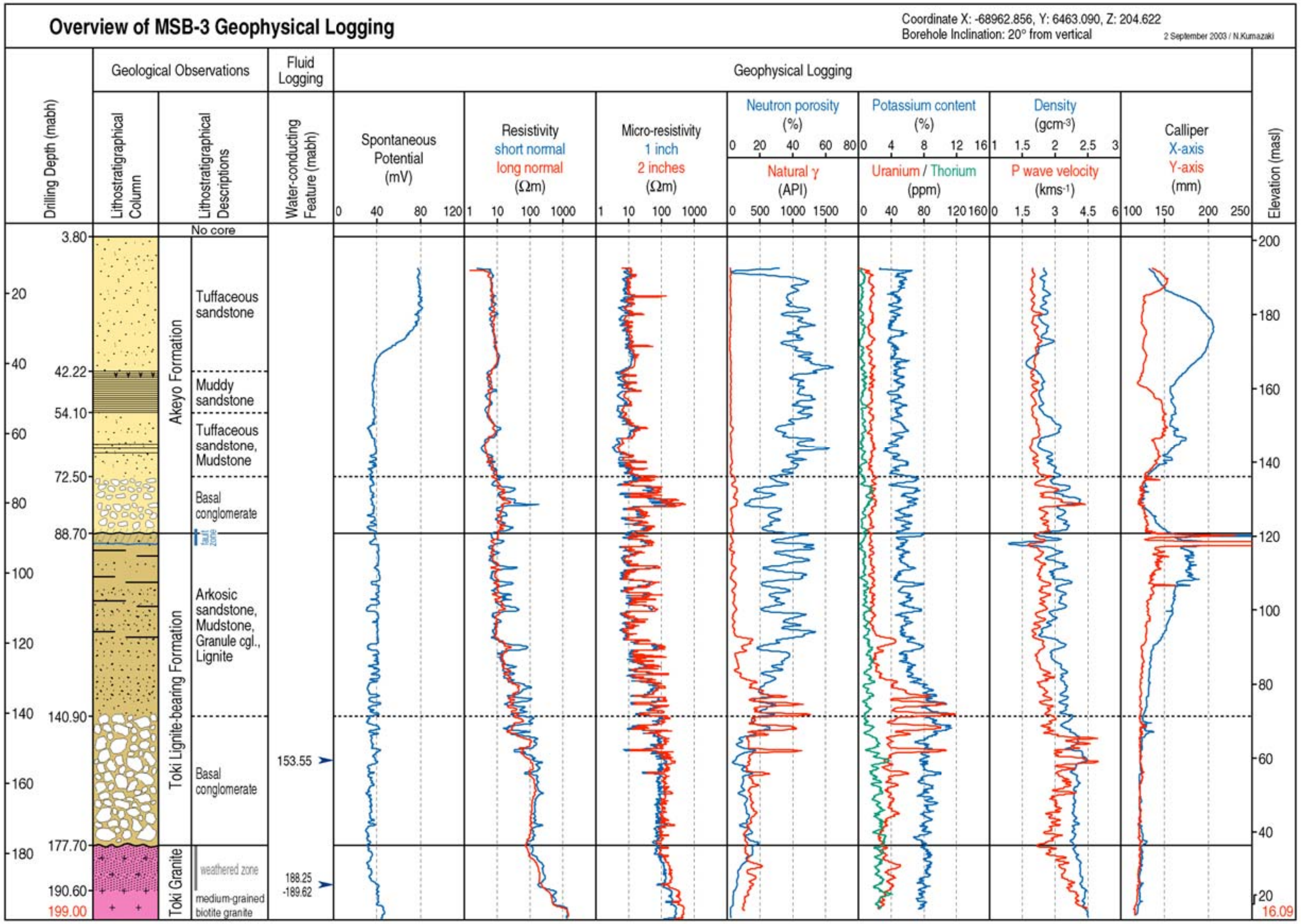

Figure 23 Overview of MSB-3 geophysical logging

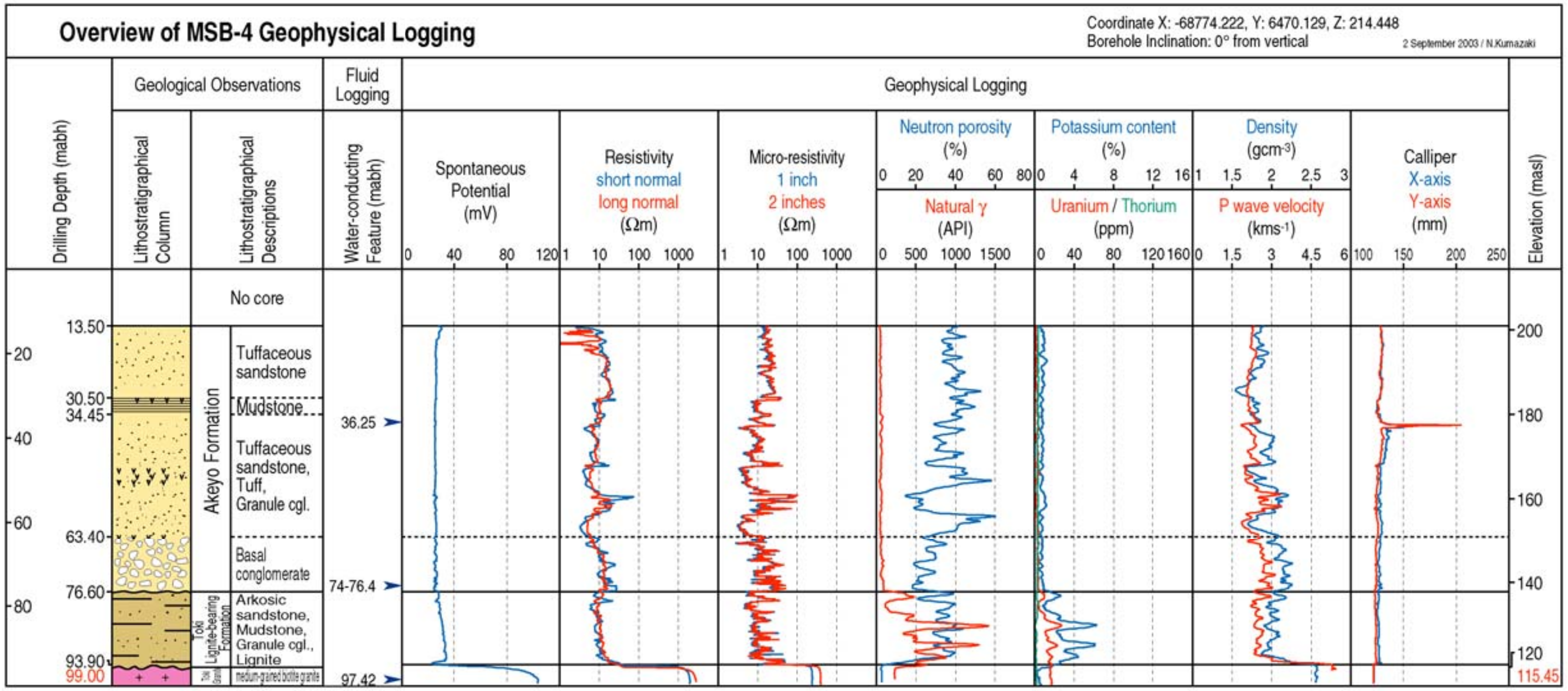

Figure 24 Overview of MSB-4 geophysical logging

BTV:

- Distributions of fracture frequency and orientation in each borehole, presented in Figures 25 and 26, were observed in BTV images and also coincided with the data from the core description.
- Subhorizontal fractures are dominant in the all sections of the sedimentary rocks and in the granite, except for the granite in MSB-4, in which steep WNW striking fractures are dominant. NS and NNW striking fractures dipping at steep angles towards the east are dominant in the weathered granite in MSB-3.
- Two fracture zones, defined by an abrupt increase in cumulative fracture frequency, were identified in the Akeyo Formation in MSB-1. In these zones, EW and NE striking fractures dipping at steep to moderate angles to the south are predominant. Also, one fracture zone was identified along the NNW fault in MSB-3, in which NW striking fractures dipping at steep to moderate angles towards the east are predominant.
- Four water-conducting features identified in MSB-1, based on fluid loss during drilling, are EW and EWE striking and dipping at steep to moderate angles towards the south or north.

2.3.4 Evaluations

- Some coarse clastic layers were identified as anomalies by the geophysical logging. However the anomaly depths did not always coincide with the depths of fluid loss during drilling nor did with the anomalies on the fluid logging.
- Although argillaceous layers were not identified, tuffaceous sandstone layers of low resistivity were defined in part of the Akeyo Formation. They are possible to be impermeable layers in the sedimentary rocks.
- Information was acquired on the orientation and geometry of many of the geological discontinuities. But we could not acquire this data for the NNW fault, and some of the fractures in the conglomerate and the weathered granite because of sludge accumulation on the borehole wall and significant enlargement of borehole diameter, making it difficult to get reliable BTV images.
- Continuous profiles of geophysical properties were acquired in each borehole to support the geological and hydrochemical modelling.
- Relevant data on in situ neutron flux production was acquired in each borehole.

2.3.5 Lessons learned

- A unidirectional scan line on core should be drawn to accurately infer the orientation of discontinuities, preparing for loss of BTV images because of sludge accumulation, borehole enlargement and turbidity of drilling fluid.
- Logging methods applicable to extremely low groundwater level (unsaturated or partially saturated conditions) should be included in working programme.
- Employment of other geophysical logging method should be considered for identification of potential water-conducting features in sedimentary rocks, because depths of anomalies from the borehole geophysics did not always coincide with the depths of fluid loss during drilling and of the fluid logging anomalies.

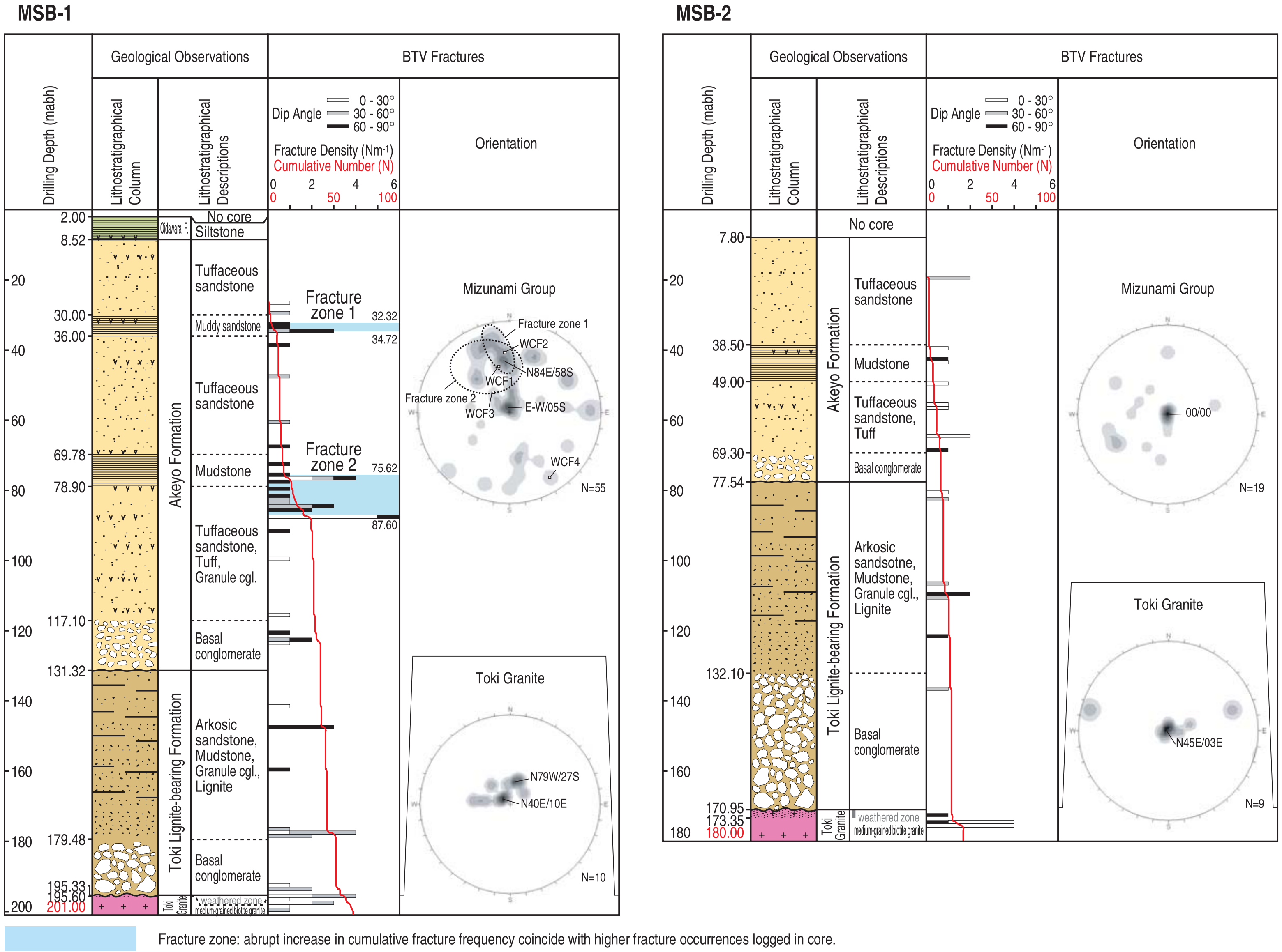

Fracture zone: abrupt increase in cumulative fracture frequency coincide with higher fracture occurrences logged in core.

Figure 25 Fracture frequency and orientation in MSB-1 and 2

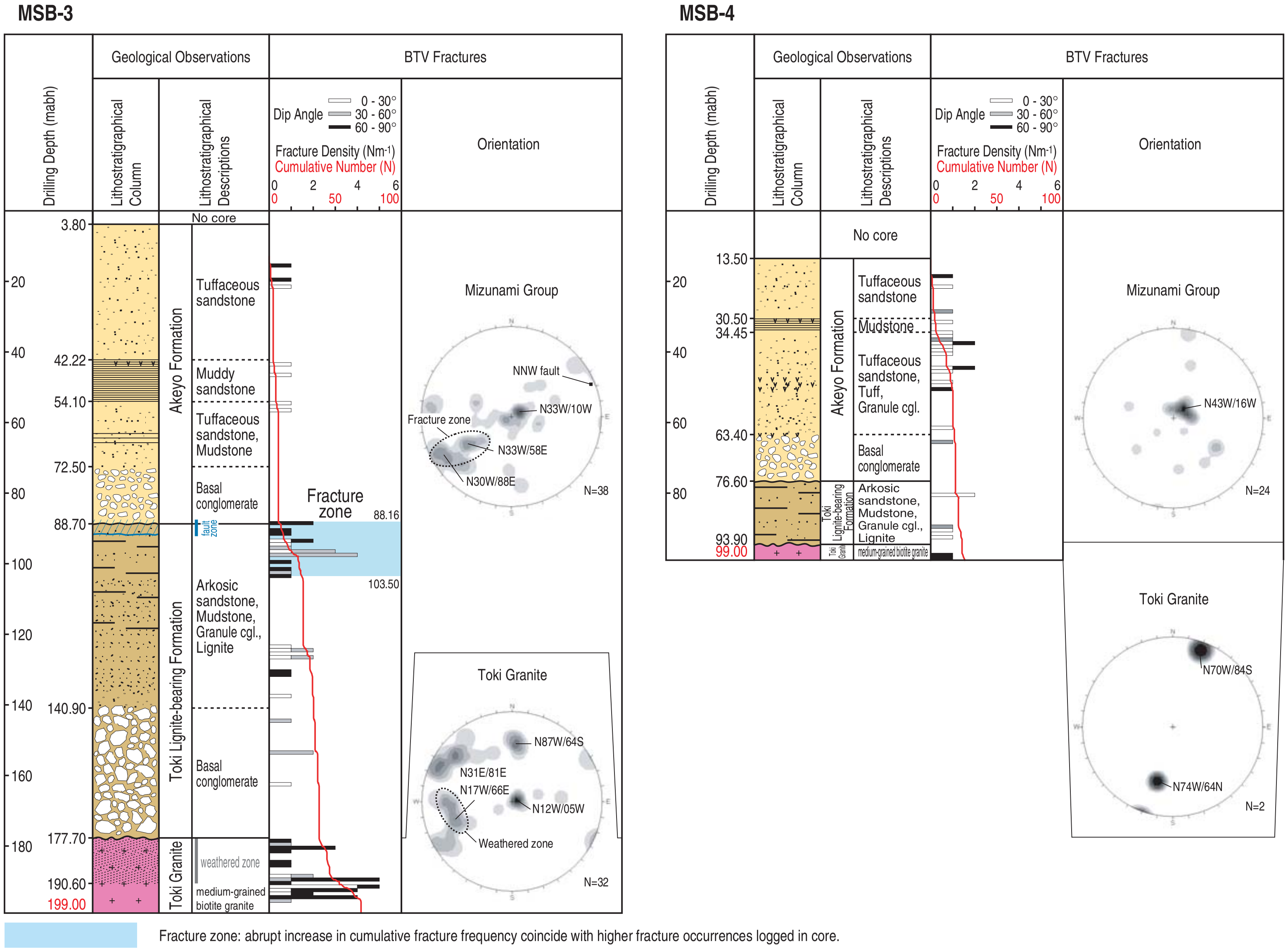

Fracture zone: abrupt increase in cumulative fracture frequency coincide with higher fracture occurrences logged in core.

Figure 26 Fracture frequency and orientation in MSB-3 and 4